

CHAPTER 3

Component Description and Modeling

Chapter 3 presents requirements and descriptions in each of component, design and reason to select components in this measuring system which consist of the air conditioning inlet section, the particle charging section, the particle size classifiers for PM10, PM2.5, and PM1.0, the particle detector with electrometer circuit which install inside Faraday cage, analog to digital and RS485 to USB port converter, personal computer, operating software flow system, power system and other accessories.

3.1 Design of the PMx Detector

The overall design goal of this work is to develop the multi-channel airborne PM detector by an electrical technique (PMx detector) that can measure PM10, PM2.5, and PM1.0 simultaneously. It should be able to report in units of the particle mass concentration and the particle number concentration, less than 1 s in processing time, more than 100 h in continuous operating time that requires no service and maintenance. Table 3.1 shows the specification of the prototype detector in this thesis. This measuring system should have small size and low price. The main assemblies can be manufactured in the local area. The operating diagram of the system is shown in Figure 3.1. This system uses the electrostatic principle for detecting charge on particle that accumulate on the high efficiency particulate air (HEPA) filter which changed according to particle mass. This system can continuous measure PM10, PM2.5, and PM1.0 simultaneously in the air. It consists of the sample inlet, the humidity removal unit, the particle charger, the particle size selector for PM10, PM2.5, and PM1.0, the particle detector with the electrometer circuit, the Faraday cage that is a main structure of the particle size selects, the particle detector, and the electrometer circuit, HEPA capsule filter, analog to digital and RS485 to USB converter, direct current (DC) low and high voltage power supply, flow meter and controller, and vacuum pump. It can draw the sampling air from the vacuum pump at 15 L/min in flow rate. The sample passes to the sample inlet and to the humidity remover

(silica gel). RH is removed with diffusion principle. Then, the air sample flows to the particle charger to receive an electric charge from the corona field inside the particle charger. The flow is separated in three channels for PM₁₀, PM_{2.5}, and PM_{1.0} classification. Each channel has 5 L/min flow rate. For the particle size of PM₁₀, the PM that are larger than 10 µm in diameter is collected on impaction plate by inertial force, but PM less than 10 µm in diameter can flow with the mainstream line to HEPA filter in the filter holder. Sheath air flows to the Rotameter and out of the system at the vacuum pump. PM_{2.5}, and PM_{1.0} use the same principle. The particle charge signal is sent to the electrometer circuit and amplifier to negative voltage signal, then the analog to digital and RS485 to USB converter transfer measuring data to the computer. The measuring data is converted into particle number and particle mass concentration by the operating software. The electric power of this system is designed based on 220VAC 50Hz. However, this system can use battery 12VDC for several hours. Specification of the PM_x detector is shown in Table 3.1.

3.2 Sample Conditioning Inlet Section

3.2.1 Requirements. This Section is separated into two parts (1) the sampling head and (2) the diffusion dryer. The sampling head was installed outside measuring station between 1.5 to 6 m in height. In addition, it has a cover and mesh for protection from rain and small insects. Sampling head must enable good air flow and be made from material that can tolerate sunlight. Humidity in ambient is an important variable that induces an error, especially during the rains. A device for removal of humidity is needed to decrease this error. This device should have high efficiency, low particle loss, low price, easy to use and maintenance.

3.2.2 Design Description. From literature reviews, sampling head of the commercial automatic PM monitor was installed on a tripod and connected tube in the vertical axis to measuring unit (Meyer et al. 2011). Figure 3.2 shows design and cross section of the sampling head. It has 6 mm diameter of 24 surrounding inlet holes. There are many holes for airflow and have a smaller mesh for insect protection. The air tube is made from the stainless and 10 mm in diameter. Figure 3.3 shows feature of the sampling head made from Delrin® material that is robust and tolerate for sunlight.

Table 3.1 Specification of the PMx detector.

Characteristic	Details
Sample inlet <ul style="list-style-type: none"> • Material • Air direction • Protection • RH control • Air tube 	For aerosol inlet <ul style="list-style-type: none"> • Delrin® • 360 degree horizontal • Small insects with mesh and rain • Diffusion technique with silica gel • PE tube 8 mm.
Particle size selector <ul style="list-style-type: none"> • Material • Particle size • Air flow rate • Type of particle 	Inertial impactor <ul style="list-style-type: none"> • Brass • PM10, PM2.5, and PM1.0 • 5 L/min (15 L/min total) • Solid and liquid
Particle collector <ul style="list-style-type: none"> • Material • Size/diameter • Filter • Cover plate 	Filter holder <ul style="list-style-type: none"> • Brass • For 47 mm in HEPA filter diameter • HEPA filter • Stainless mesh
Particle sensor <ul style="list-style-type: none"> • Material • Amplifier • Bias current • Signal filter • Feedback resistor 	<ul style="list-style-type: none"> • Brass for Faraday cage • Op-amp LMC6032 • 40×10^{-15} fA • Low pass filter circuit for 7.23 Hz • 500 GΩ
Controller and data processor <ul style="list-style-type: none"> • Data converter • Number of input data • Display and report • Processing time • Connector/port 	Personal computer <ul style="list-style-type: none"> • ADAM 4017 for ADC 16-bit • 3 channels for PM10/PM2.5/PM1.0 • Computer displays • Less than 1 s • UCON 485 for USB converter
Computer software <ul style="list-style-type: none"> • Operating system • Display • Remote controller • Data logger 	<ul style="list-style-type: none"> • Windows XP or higher • Dynamic graph • Team viewer software • Dropbox software and hard disk drive
Particle number concentration range	10^{10} to 10^{14} particles/m ³
Mass concentration range	500 µg/m ³
Power supply	220 VAC 50Hz and 12 VDC for reserve
Operating time	More than 100 h (After clean)

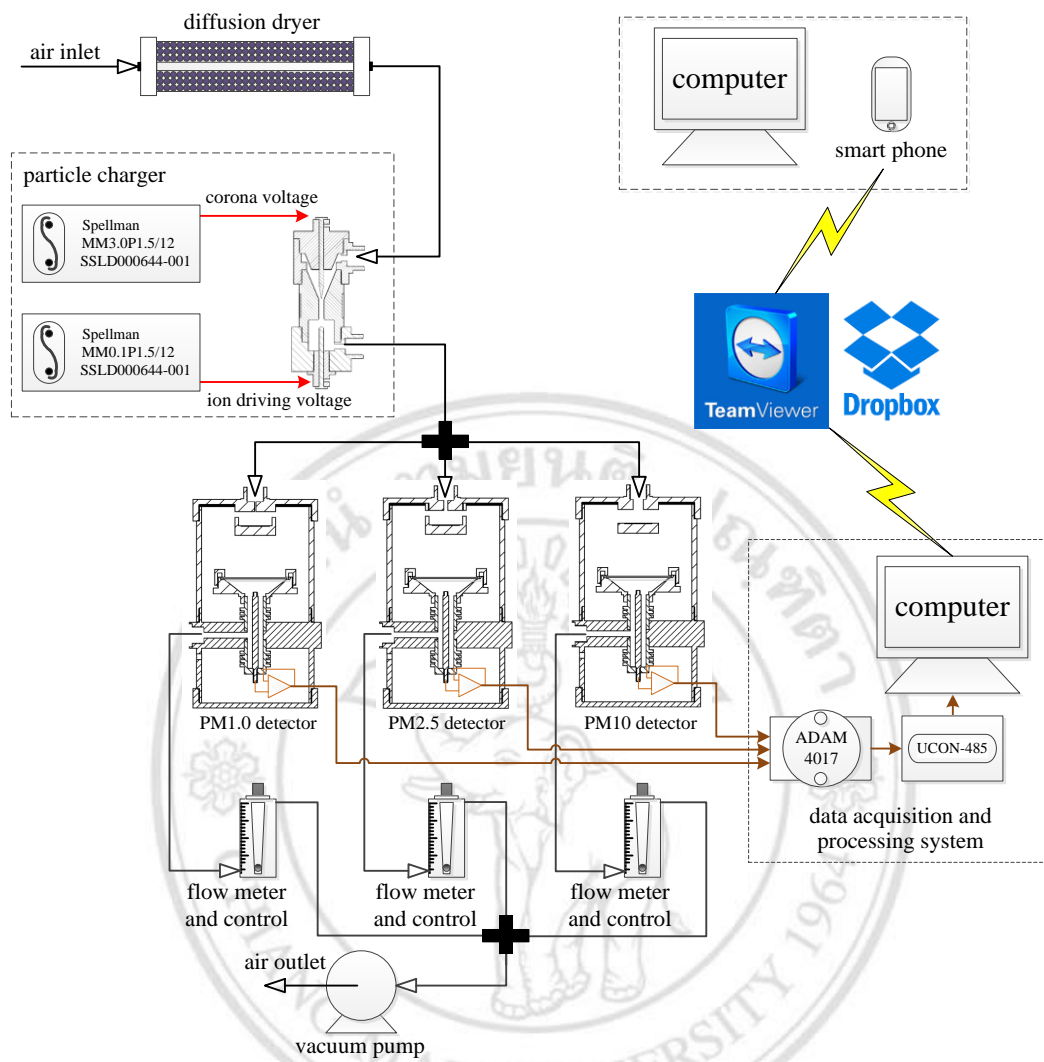
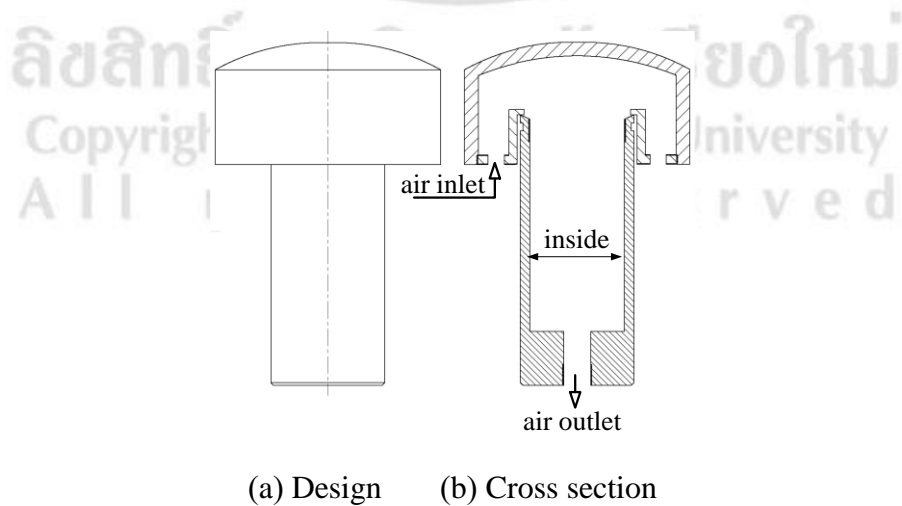


Figure 3.1 Operating diagram of the PM_x detector.



(a) Design (b) Cross section

Figure 3.2 Design and cross section of the sampling head.



Figure 3.3 Feature of the sampling head.

Nafion technique used for absorbing the RH or water from the air samples has the heat exchange system inside (Perma Pure 2000). A sample is condensed with low temperature purge gas, then the water will stick on a tube wall and permeate out with the purge gas. This system needs a heat source for increasing the temperature of air sample to higher than the dew point. It can be used at 120 °C operating temperature and 80 psig, and has a dew point temperature down to -40 °C. The diffusion drying technique was used for absorbing liquid from aerosol sample. Absorbent material used was silica gel or activated carbon. Aerosol diffusion dryer (Cambustion 2017) of Cambustion Company used for decreasing the RH from the air sample at about 4 L/min in aerosol flow rate, similar to the diffusion dryer model 3062 of the TSI Company (TSI Company 2017). TSI 3062 is used for absorbing vapor of aerosol from the aerosol generator or atomizer that has water trapped inside. Silica gel packed around the central mesh tube can absorb humidity by diffusion. This method has a low particle loss. The silica gel can be baked at 120 °C for reuse. TSI3062 can decrease humidity from 60% RH at inlet down to 20% RH. Diffusion dryer model DDU570 of TOPAS Company (TOPAS 2016) was 7 cm in diameter, 47.5 cm in length and used for 0 - 4 L/min in aerosol flow rate. DDU570 was designed for absorbing humidity from an aerosol of aerosol generator ATM model 220. DDU570 can be used at temperature more than 1,000 °C. DDU570 can be used continuously for three days, then silica changed from orange to light color when fully absorbed. Diffusion dryer model DD250 of ATI (ATI Company 2017) has 5.67 cm in diameter, 28.2 cm in length, 415 kPa (60 psig) in maximum pressure, used for 0 - 4 L/min in aerosol flow rate and can pack silica gel at 0.25 kg (total weight at 0.57 kg). DD250 use silica gel for absorbing humidity. Central tube inside is made from stainless mesh and

has silica gel around it which shrouded by stainless mesh. The outer cylindrical tube was glass. End caps were made from Delrin® and can be removable for packing a silica gel. DD250 can dehumidify for 60% RH inlet down to 21 % RH and 23% RH for over 3 h operating or 80% RH inlet down to 22 % RH and 27% RH for over 3 h operating. DMT diffusion dryer from Droplet Measurement Technologies; DMT Company (DMT Company 2017) used a silica gel or activated charcoal for absorbing humidity. It has a screw cap that can be removable for packing absorbed material. The stainless mesh tube has 1.5 mm inside hole diameter and has 2 sizes in 38.1 cm and 60.96 cm in length.

A humidity reduction device for automatic PM monitor commonly uses Nafion and diffusion drying technique as shown in Table 3.2. The diffusion technique uses for low flow rate, while the Nafion® technique uses for high flow rate and popular used for TEOM (Meyer *et al.* 2001). But, it has a high price and complex system. Tuch *et al.* (2009) developed the automatic aerosol dryer for 16.67 L/min air flow by the diffusion technique which was possible to increase the air flow rate by diffusion length and volume of silica gel. Figure 3.4 (a) shows the design and a cross section of the diffusion dryer for the sample inlet in this thesis. It has 32 mm inner diameter, 90 mm in outer diameter and 1,000 mm in length. Figure 3.4 (b) shows features of the diffusion dryer which the inside tube made from stainless mesh and the outside tube made from acrylic transparent. This RH removal can contain a silica gel up to about 5 kg. Silica gel turns from blue to pink when used for a long time. It can be removed and reloading for a new silica gel.

3.2.3 Analytical Models. The velocity (v) of air flow at inlet, inside and outlet at the sampling head were calculated from the flow rate and the flow area ($v = Q / A$). The inside velocity was needed to use to define the numerical model section. This device had 15 L/min, which was $2.5 \times 10^{-4} \text{ m}^3/\text{s}$ in air flow rate. While, the air velocity inside the diffusion dryer had 15 L/min, which can be calculated to be $2.5 \times 10^{-4} \text{ m}^3/\text{s}$.

3.2.4 Numerical Models. Numerical simulation is needed for validating internal flow field, electric field and particle trajectories in all devices. The sampling head, the diffusion dryer, the particle charger, the particle size selector and the particle charge detector were designed in cylindrical shape. So we can use 2D for finding flow field, electric field and particle trajectory model. 2D incompressible Navier-Stoke equations

Table 3.2 Comparison of the diffusion dryer and Nafion products.







Item	Model/Manufacturer	Type	Characteristic
1	Cambustion aerosol diffusion dryer 	Diffusion dryer used a silica gel or activated carbon	<ul style="list-style-type: none"> • Used for removing liquid from aerosol particle • Absorbs material place the block for aerosol samples • 9 cm of diameter • 21.5 cm in length • 1.55 kg in weight (total)
2	Diffusion dryer model 3062 	Diffusion dryer	<ul style="list-style-type: none"> • Used for aerosol generator or atomizers • Absorbs material place beside the aerosol tube for low particle loss • Can reduce humidity from material absorbs by oven (about 120°C) • 3 kg in weight (total) • About 2,550 USD in price • 415 kPa in maximum pressure • 0 – 4 L/min in aerosol flow rates
3	Diffusion dryer model DDU 570 	Diffusion dryer	<ul style="list-style-type: none"> • Used for aerosol generator or atomizers • Absorbs material place the block for aerosol samples • 7 cm in length • 47.5 cm in length for DDU570/H model and 25.3 cm in length for DDU570/L • Melting point >1,000°C • 0 – 4 L/min in aerosol flow rates
4	Diffusion dryer model DD250 	Diffusion dryer	<ul style="list-style-type: none"> • Absorbs material place the block for aerosol samples • 3 h continuous operation • Absorbs material place beside the aerosol tube for low particle loss • Decrease humidity from 60%RH down to 21%RH (under 3 h operating) and 23%RH (over 3 h operating) • Decrease humidity from 80%RH down to 22%RH (under 3 h operating) and 27%RH (over 3 h operating) • 5.67 cm in diameter and 28.2 cm of length • 0.57 kg in weight (body only) • 415 kPa in maximum pressure • 0 – 4 L/min in aerosol flow rates

Table 3.2 (con.) Comparison of the RH removal products from diffusion dryer and Nafion technique

Item	Model/Manufacturer	Type	Characteristic
5	DMT Diffusion dryer of DTM Company 	Diffusion dryer	<ul style="list-style-type: none"> Absorbs material placed beside the aerosol tube for low particle loss 38.1 cm and 60.96 cm diameters
6	MD series gas sample dryers by Perma Pure LLC Company 	Nafion®	<ul style="list-style-type: none"> Heat exchange of aerosol samples and temperature lower than the dew point for condense to liquid on Nafion and can continuously operate Nafion inner 1.07 – 2.18 cm in diameter Nafion outer 1.35 – 2.74 cm in diameter 30.48 – 365.76 cm in length 120 °C in operating temperature 80 psig in maximum pressure 0 – 4 L/min in aerosol flow rates
7	PD series gas sample dryers by Perma Pure LLC Company 	Nafion®	<ul style="list-style-type: none"> Heat exchange of aerosol samples and temperature lower than the dew point for condense to liquid on Nafion and can continuously operate 1.91 – 2.54 mm of Nafion diameter 120°C in operating temperature 80 psig in maximum pressure 0 – 40 L/min in aerosol flow rates
8	Meyer <i>et al.</i> (2010)	Nafion®	<ul style="list-style-type: none"> 3 L/min in aerosol flow rates Continuously operates The bypass flow line consisted of 50 tubes of 0.635 mm ID The sample stream dryer consisted of 18 tubes of 1.524mm ID
9	Tuch <i>et al.</i> (2009)	Diffusion dryer	<ul style="list-style-type: none"> Automated aerosol diffusion dryer Used for 16.67 L/min in aerosol flow rates 160 kg in total weight Two parallel stainless steel columns with 70 mm inner diameter and 800mm in total length Each of columns approximately 11 kg with Silica gel Stainless steel mesh at 0.25 mm wire diameter

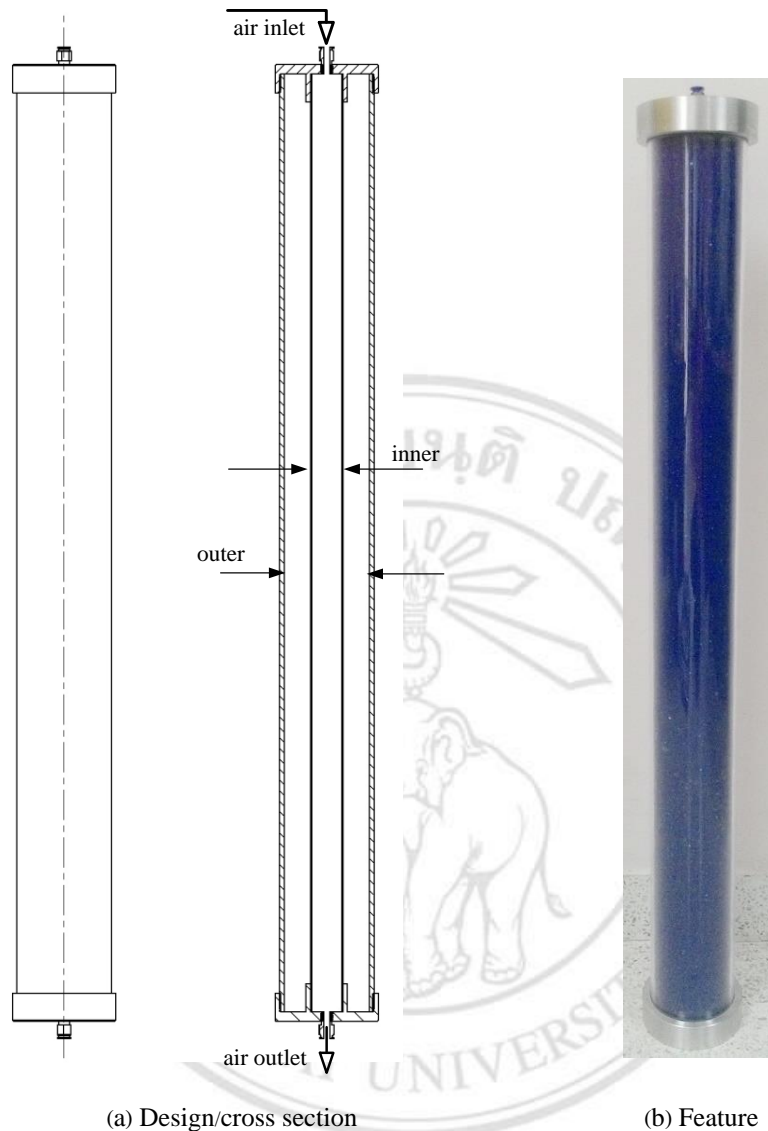


Figure 3.4 Design/cross section and feature of the diffusion dryer.

were selected for numerical simulation of the internal flow. It can be written in partial differential equation (PDE) in the cylindrical coordinate system.

1) Governing Equations for the Air Flow. COMSOL is a simulation software for flow analysis of this component. Incompressible Navier-Stokes model equations from COMSOL shown in Eqs. (2.86) and (2.88) were applied in this analysis. The condition for this simulation was set at 60% in the RH and 30 °C of room temperature at 320 m from sea level (DoiSaket Chiang Mai). Simulation variables were 1.107 kg/m³ in air density, 1.343×10⁻⁵ Pa.s in air dynamic viscosity, 303.15 Kelvin in internal temperature and 1 ATM for absolute pressure.

2) Governing Equations for the Particle Trajectories. For validation of particle trajectories, Khan and Richardson equation and electrostatic field from Eqs. (2.90) to (2.97) were applied. Charge and mass of particle were set as Table 2.2, corresponding to PM10, PM2.5, and PM1.0.

3) Computational Domain and Boundary Condition. The sampling head and diffusion dryer used Navier-Stokes (ns) model equations to find flow fields inside. Both models had 10 mm in outlet diameter, which is $7.85 \times 10^{-5} \text{ m}^2$ in area so from $v = Q/A$ the outlet velocity was 3.185 m/s (uniform velocity profile) at 15 L/min in air flow rate. Figure 3.5 (a) shows the computational domain of the sampling head. Figure 3.5 (b) shows boundary conditions of the sampling head. The air outlet boundary was set for the inlet boundary in COMSOL at -3.185 m/s because it was a vacuum. Figure 3.6 (a) shows the computational domain of the diffusion dryer. Figure 3.6 (b) shows boundary conditions of the diffusion dryer.

3.3 Particle Charging Section

3.3.1 Requirements. This device was used to impart a charge to the particle by field and diffusion charging, which is a positive unipolar ion type. A particle charger was used to generate high ion concentration in attaching particle surface. Good particle charger must generate high concentration ions (N_i ; more than 10^{12} ions. s/m^3), have low particle loss, long mixing time (or residence time) in charging zone, can remove free ions after charging process, and can charge particle in wide size range (PM10, PM2.5, and PM1.0).

3.3.2 Design Description. Field charging is normally used for particles larger than $1 \mu\text{m}$ in diameter. Submicron particles are appropriate with diffusion charging (Wiedensohler *et al.* 1994; Camata *et al.* 2001; Stommel *et al.* 2005; Alguacil *et al.* 2006; Park *et al.* 2011).

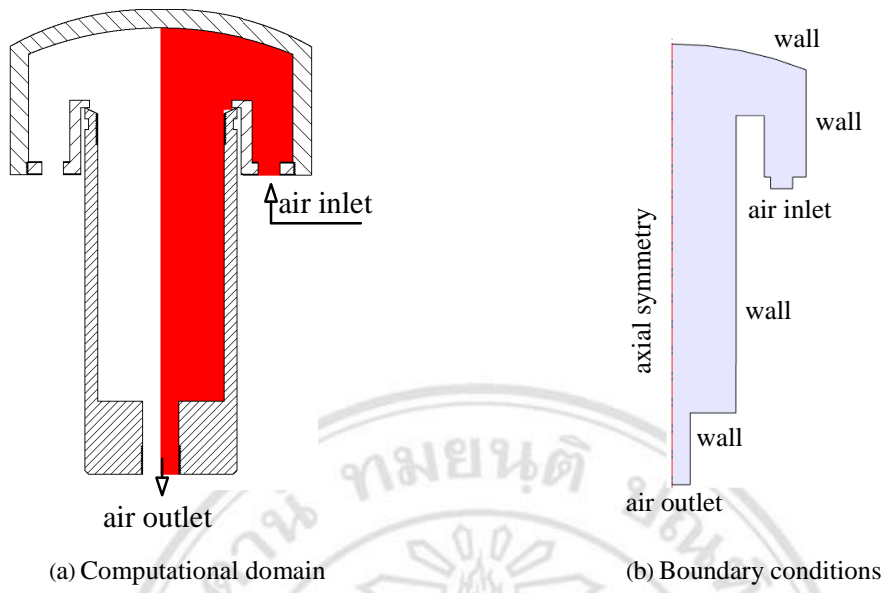


Figure 3.5 Domain and boundary of the sampling head.

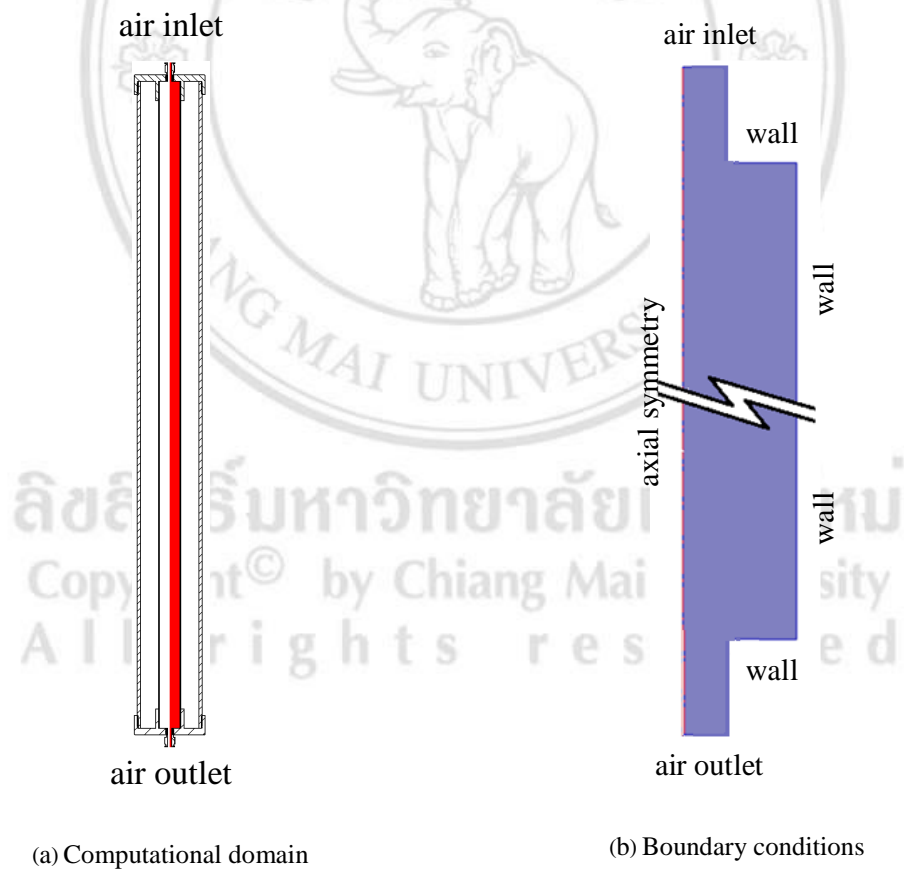


Figure 3.6 Domain and boundary of the diffusion dryer.

Although wire type charger can generate high concentration ions appropriate for large size and long residence time, it has high particle loss. The corona discharge by the needle in cone type has both field and diffusion charge (Hernandez-Sierra *et al.* 2003; Alguacil *et al.* 2006; Chien *et al.* 2011; Domat *et al.* 2014; Intra and Tippayawong 2011, 2013). This corona charger type has a higher ion concentration than the wire in cylindrical tube type from previous versions of the corona charger (Intra 2012; Intra *et al.* 2015), while the needle in cone type that separated the particle mixing zone from the ion generate zone is used to charge submicron particles (Qi *et al.* 2007, 2008; Kimoto *et al.* 2010; Li *et al.* 2011; Intra and Tippayawong 2011). The needle in cone type is popular, simple, noncomplex, robust and appropriate for PM10, PM2.5, and PM1.0. The needle in the cone was applied in this work and has the ion trap for remove the ions after charging process (Intra and Tippayawong 2011; Intra *et al.* 2014). Figure 3.7 shows the structure of the corona needle charger. The corona needle electrode was made from stainless steel connected to the high voltage direct current power supply (HVDC) and used to generate high concentration ions. Outer electrode was made from brass. Inlet and outlet were connected to air fitting PT1/8 for PE tube, as shown in Figure 3.8.

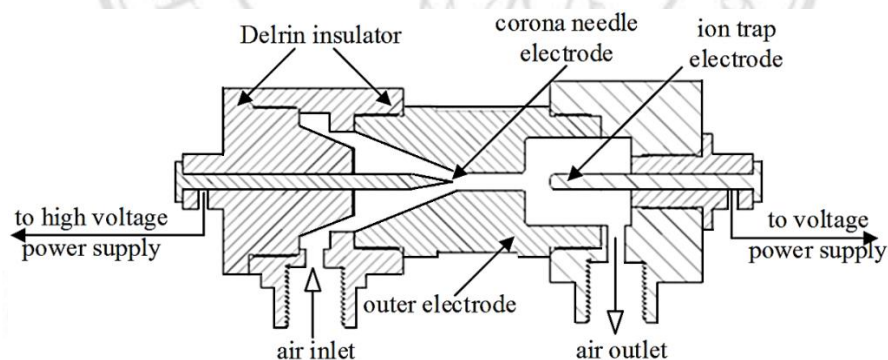


Figure 3.7 Cross section and Structure of corona needle charger.

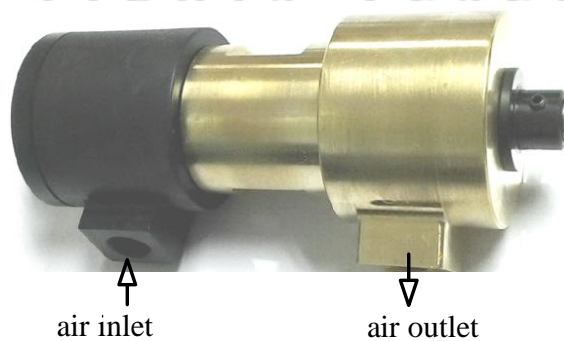


Figure 3.8 Feature of the corona needle charger.

3.3.4 Analytical Models

1) Ion Current Density. Ion current density (J) is a function of the space charge density (ρ), the ion electrical mobility (Z_i) are $1.150 \times 10^{-4} \text{ m}^2/\text{V.s}$ and $1.425 \times 10^{-4} \text{ m}^2/\text{V.s}$ for positive and negative, respectively (Reischl *et al.* 1996), and the electric field (E) which has relation in Eqs. (3.1). In addition, the current density can be written in the ion current format that flow through the inner surface area (I_{in}) of the particle charger as shown in Eqs. (3.2), where A is the inner surface of the particle charger.

$$J = \rho Z_i E \quad (3.1)$$

$$\frac{I_{in}}{A} = \rho Z_i E \quad (3.2)$$

2) Estimation of the $N_i t$ Product. The $N_i t$ can be calculated from Eqs. (3.3) to (3.5). This charger is the corona needle charger type. The radius of this charger is 0.00175 and 0.00525 m in r_1 and r_2 , respectively, while the needle length (L_1) is 0.00855m. So the charger area can be calculated as $2.03 \times 10^{-4} \text{ m}^2$. The electric field (E) can be found from the numerical model in Section 3.3.4. Particle number concentration (N_p) for the corona needle charger, shown in Figure 3.9 can be calculated from Eqs. (3.6) where I_p the discharge current (A) from the charger, n_p is the average number of elementary charges (assume at 1 electron), and Q_a is the air flow rate (m^3/s). (Intra *et al.* 2016).

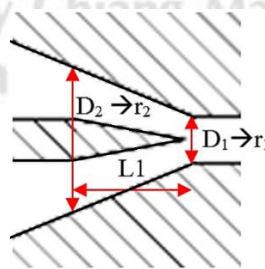


Figure 3.9 Cross section of corona needle-cone charger.

$$N_i = n_{in} = \frac{I_{in}}{e \cdot Z_i \cdot E \cdot A} \quad (3.3)$$

$$A = \pi(r_1 + r_2)\sqrt{(r_1 - r_2)^2 + L^2} \quad (3.4)$$

$$t = \frac{Volume}{Q_a} = \frac{\pi L(r_1^2 + r_1 r_2 + r_2^2)}{3Q_a} \quad (3.5)$$

$$N_p = \frac{I_p}{n_p \times e \times Q_a} \quad (3.6)$$

3) Estimation of the Particle Penetration and Loss. The ion number concentration at the output can be calculated from Eqs. (3.7) where Q is volumetric air flow though the Faraday cups (m^3/s). The ion penetration mean efficiency of charger which can be calculated from Esq. (3.8). Most of the particle loss was found in corona discharge in the charge. In addition, another loss included the gravitational loss, the space charge loss, and the diffusion loss. The electrostatic loss was defined by the ratio of the outlet and the inlet of particle concentration as shown in Eqs. (3.9) which is Deutsch - Anderson equation, where P_p is the particle penetration of the charger and can be calculated from Eqs. (3.10) (Hinds 1999).

$$n_{out} = \frac{I_{out}}{e \cdot Q} \quad (3.7)$$

$$P = \frac{n_{out}}{n_{in}} \times 100\% \quad (3.8)$$

$$loss_{elec} = \frac{N_{out}}{N_{in}} = 1 - P_p \quad (3.9)$$

$$P_p = \exp\left(\frac{-Z_p \cdot E \cdot A}{Q}\right) \quad (3.10)$$

3.3.4 Numerical Models. The particle charger used 2D Navier-Stokes (ns), electric current and electrostatic model equations to find flow field, electric field and particle trajectories, respectively. The computation area inside the charger is shown in Figure 3.10. This model can simulate together with electric current and electrostatic model. The

outlet at ion trap zone of the charger domain has 1.5×10^{-3} m and 8.75×10^{-3} m for inner and outer radius, respectively. From $v = Q/A$, the ring area outlet can be calculated 2.33×10^{-4} m².

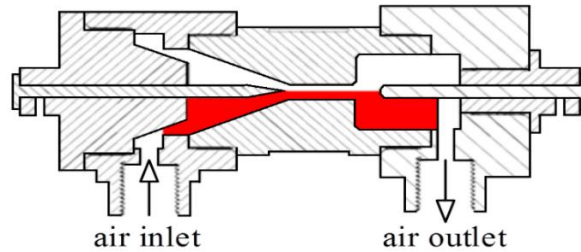


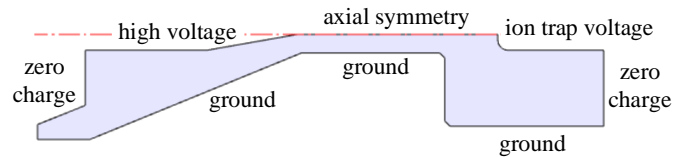
Figure 3.10 Computational domain of the charger.

1) Governing Equation for the Electrostatics. Electric current and electrostatic model equation form Eqs. (2.90) to (2.94) were used to validate electric field and electrostatic force. The simulation variables were 1.00059 for relative permittivity of air and 5×10^{-15} S/m for electric conductivity of air.

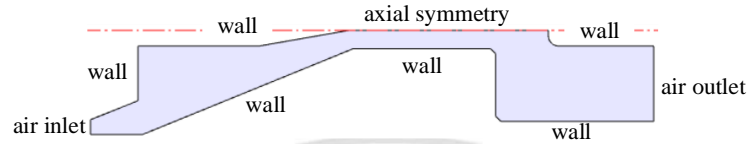
2) Governing Equation for the Air Flow. Incompressible Navier-Stokes model equations from COMSOL as shown in Eqs. (2.86) and (2.89) were applied in this analysis. The condition for this simulated were set at 60% RH and 30 °C of room temperature at 320 m from sea level (DoiSaket Chiang Mai). Simulation variable were 1.107 kg/m³ in air density, 1.343×10^{-5} Pa.s in air dynamic viscosity 303.15 Kelvin in internal temperature and 1 ATM for absolute pressure. This charger model used 15 L/min or 2.5×10^{-4} m³/s of particle flow rate and can be calculated 1.073 m/s in outlet particle velocity. The particle outlet was set at 1.0714 m/s (but set inlet at -1.073 m/s in COMSOL).

3) Governing Equation for the Particle Trajectories. Electric current and electrostatic field from Eqs. (2.90) to (2.94) Khan and Richardson equation from Eqs. (2.95) to (2.97) were applied to validate the particle trajectories inside the charger. Charge of particle was set as Table 2.2, corresponding to PM10, PM2.5, and PM1.0.

4) Computational Domain and Boundary Condition. Figure 3.10 shows the computational domain of this charger. Figure 3.11 (a) and (b) show boundary conditions of electric field and flow field, respectively. Computation condition for numerical model is shown in Table 3.3.



(a) Electric field boundary.



(b) Flow field boundary.

Figure 3.11 Boundary conditions of the charger.

3.4 Size Classification, Faraday Cups and Cage

3.4.1 Requirement

1) **Size Classification.** This part is used for selection of particles less than 10, 2.5, and 1.0 μm in diameter for PM10, PM2.5, and PM1.0, respectively. This electrical PM monitor must be able to measure PM10, PM2.5, and PM1.0 simultaneously. Air flow rate of 5 L/min in each of classifying channels was used with 15 L/min in main flow rate. The classifier should be able to operate continuously, long lifetime, easy to install and maintenance and low electrostatic effect. In addition, this part should be near Faraday cups to reduce particle loss and should be made from an electricity conductive material to reduce electric charge effect of particles.

Table 3.3 Computation condition for numerical model.

Operation condition	Details
Voltage at a corona needle electrode	2.0 – 3.0 kV
Voltage at an ion trap electrode	0 and 300 V
Outlet gas velocity	1.073 m/s
Flow characteristics	Laminar
Particles flow rate	15 L/min or $2.5 \times 10^{-4} \text{ m}^3/\text{s}$
Gas density	1.107 kg/m ³
Gas dynamic viscosity	$1.343 \times 10^{-5} \text{ Pa}\cdot\text{s}$
Relative permittivity of gas	1.00059
Operating temperature	303.15 Kelvin
Electrical conductivity	$5 \times 10^{-15} \text{ S/m}$

2) Faraday Cup. Signal measurement of electric current in this thesis is done by Faraday cup. Particle number concentration can be calculated from Eqs. (2.56) which converts 10 fA electric current to 6.747×10^5 , 9.653×10^6 , and 5.159×10^7 particles/ m^3 from PM10, PM2.5, and PM1.0, respectively (at 17% ion penetrations and have number of elementary charges from Table 2.2). Faraday cups should collect all particles and send an electric charge to the electrometer circuit to convert to electrical signals. In addition, it should be easy to install and maintain. The charge on particles was very low, which has high sensitivity from an interfering signal, so, it required Faraday cage for this protection.

3) Faraday Cage. Faraday cup is highly sensitive for any electric charge and interfering signal. It needs to have a Faraday cage to protect the interfering signal. Faraday cage should be made from good conductor material, robust, durable, easily installed and quick maintenance for Faraday cups inside. In addition, it can send the ultra-low current from the Faraday cups to the electrometer circuit without loss.

3.4.2 Design Description

1) Size Classification. The impactor uses a gravimetric method for classifying and separating particles. This method is well defined by US EPA. An impactor technique in Figure 2.10 is used for particles between 0.1 to 50 μm in diameter. An inertial impactor in Section 2.1.8 is noncomplex and easy to operate. Nozzle jet and impaction plate were designed for cut size of less than 1.0, 2.5, and 10 μm in diameter. From Section 2.1.8, the inertial impactor was designed for 5 L/min air flow rate and assuming that the particles have a spherical shape. The nozzles diameter were calculated that 6.5, 2.6, and 1.5 mm and have 1080, 2701, and 4681 in Reynold number of PM10, PM2.5, and PM1.0 respectively (Marple and Willeke 1976; Hinds 1999; Willeke and Baron 1993; Intra *et al.* 2010, 2012, 2013, 2016).

The impactor in DustDETEC version 1.0 shown in Figure 3.12 is a design for installing at the sampling head. The particles after size classification may be loss in tube between this part and Faraday cup. The impactor in this thesis was designed to be inside a Faraday cage near Faraday cups to reduce particle loss. Feature of inertial impactor in

this thesis is shown in Figure 3.13 (a), (b), and (c) for PM10, PM2.5, and PM1.0, respectively. In addition, the impactor in DustDETEC version 1.0 was made from Delrin® material, which was not conductive and should have an electrostatic effect on the surface. The impactor in this thesis was made of brass material for low electrostatic effect, as shown in Figure 3.14.

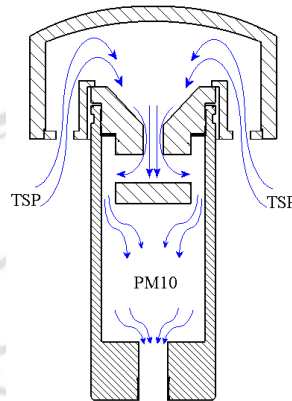


Figure 3.12 Cross section of PM10 impactor of DustDETEC version 1.0 (Intra and Yawootti 2012).

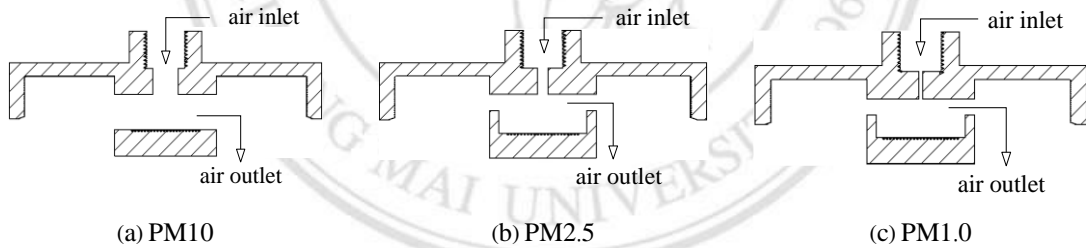


Figure 3.13 Cross section of the inertial impactor.



Figure 3.14 Feature of the inertial impactor.

2) Faraday Cup. Faraday cup of DustDETEC version 1.0 was made from stainless material which get particles at inlet on top and diffuse on the surface of the HEPA filter. The mesh pressing the HEPA filter was made from aluminum grooving material as shown in Figure 3.15 (a). Faraday cup used brass material because it was

lighter, cheaper and a good conductor. Figure 3.15 (b) shows Faraday cups that made from brass material and uses a small mesh to press the HEPA filter.



Figure 3.15 Characteristic of Faraday cups and HEPA filter.

Figure 3.16 shows the components of the Faraday cup which contained a HEPA filter 47 mm in diameter for collecting samples and total charge from the PM. The HEPA filter was put on the base mesh of the holder and had a press mesh on top. The holder was on Teflon® insulator for isolation and protection from ultra-low signal from ground base. QM-A quartz filter circle of the Whatman Company was applied. It was used for sampling and collecting particles larger than 0.3 μm in diameter.

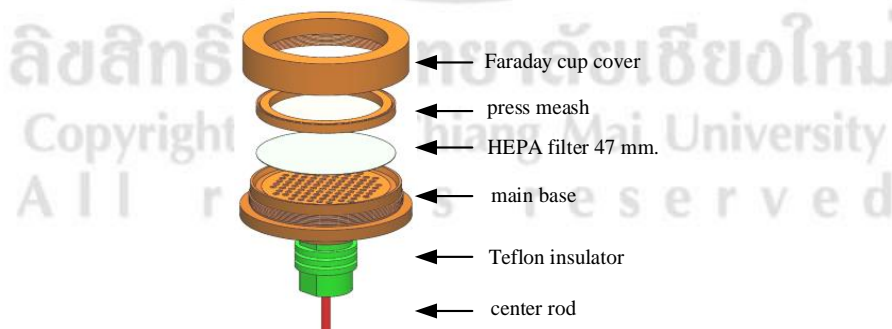


Figure 3.16 Components of the Faraday cup.

3) Faraday Cage. Faraday cage was designed in a cylindrical shape corresponding with the size classification and Faraday cup. In addition, it was made from brass material and was designed for connection between the size classification and

Faraday cup. Three Faraday cages as shown in Figure 3.17 were used as shown in Figure 3.18, but different at the PM size classification.

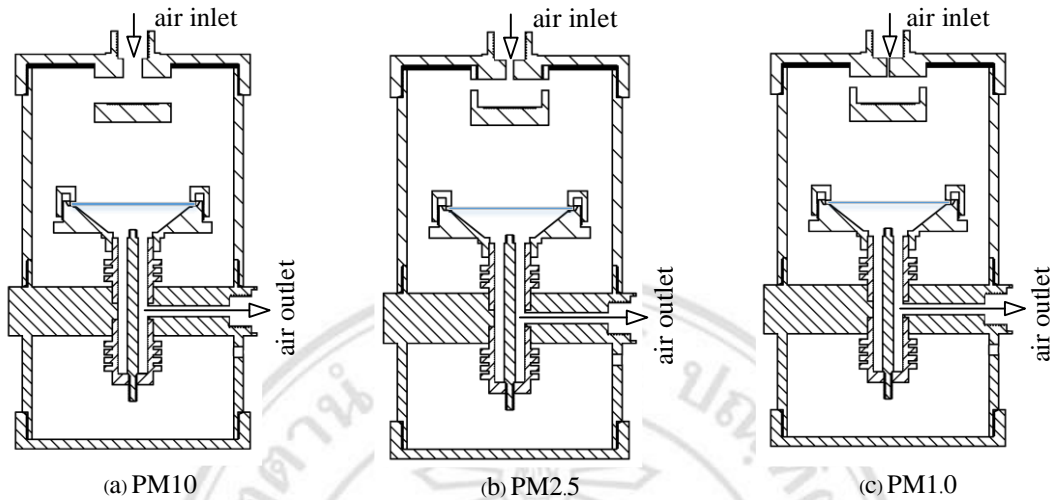


Figure 3.17 Cross section of Faraday cage.



Figure 3.18 Feature of the Faraday cage.

3.4.3 Analytical Models

1) PM10, PM2.5, and PM1.0 Classification. Diameter of nozzles can be calculated from the Stoke number (Stk). Stoke number is a dimensionless parameter that describes the nature of impaction. Stokes equation is shown in Eqs. (3.11), where ρ_p is the particle concentration, C_c is Cunningham compensator, d_p is the particle cutoff diameter, V is the average velocity at the nozzle, η is gas viscosity, and D is the nozzle diameter. The average velocity can be calculated from Eqs. (3.12). The Eqs. (3.12) and

Eqs. (3.11) resulted in a new equation as shown in Eqs. (3.13). Eqs. (3.13) can calculate the particle cutoff diameter at 50% collection efficiency (d_{50}) as shown in Eqs. (3.14) (Hinds 1999). Because the Cunningham compensator is a function of diameter, Eqs. (3.14) cannot calculate in normal method, so that d_{50} can be estimated from $d_{50}\sqrt{C_c}$ by the empirical equation as shown in Eqs. (3.15). This equation has 2% accuracy for $d_{50} > 0.2\mu m$ and between 0.9 – 1 bar in system pressure, so that the nozzle diameter can be calculated from Eqs. (3.16), where Stk_{50} is the Stoke number of particles at 50% collection efficiency and has 0.24 for the 1.0 in the ratio of the nozzle diameter and distance from the nozzle to the impaction plate (Hinds 1999; Marple and Willeke 1976).

$$Stk = \frac{\rho_p C_c d_p^2 V}{9\eta D} \quad (3.11)$$

$$V = \frac{Q}{A} = \frac{4Q}{\pi D^2} \quad (3.12)$$

$$Stk = \frac{4\rho_p C_c d_p^2 Q}{9\pi\eta D^3} \quad (3.13)$$

$$d_{50} = \sqrt{\frac{9\pi\eta D^3 Stk_{50}}{4\rho_p Q C_c}} \quad (3.14)$$

$$d_{50} = d_{50}\sqrt{C_c} - 0.078 \times 10^{-6} \text{ for } d_{50} \text{ in meter unit} \quad (3.15)$$

$$D = \sqrt[3]{\frac{4\rho_p (d_{50}\sqrt{C_c})^2 Q}{9\pi\eta Stk_{50}}} \quad (3.16)$$

2) Collection Efficiency. The Particle penetration efficiency (P) of the particle size classification can be calculated from Eqs. (3.17) where η is the particle collection efficiency (E_c) of the classificatory which be found from Eqs. (3.18) (Kuo and Tsai 2001).

$$P = (1 - \eta) \times 100 \quad (3.17)$$

$$E_c = \frac{1}{1 + (d_{50} / d_p)^2} \quad (3.18)$$

3.4.4 Numerical Models

1) **Governing Equation for the Air Flow.** The velocity at the inlet of the particle size classifier was used for defining the numerical model in the next section. All three size classifiers have 5 L/min or $8.333 \times 10^{-5} \text{ m}^3/\text{s}$ in air flow rate. The impactors had 6.5, 2.6, and 1.5 mm in inlet hold diameter for PM10, PM2.5, and PM1.0, respectively. They were calculated to be 2.51, 15.69, and 47.16 m/s for inlet air velocity of PM10, PM2.5, and PM1.0, respectively. The cups of three impactors had $28 \times 10^{-3} \text{ m}$ in diameter and can be calculated as $8.797 \times 10^{-4} \text{ m}$ in circumference. The outlet area of the PM10 impactor cup were 8.797×10^{-4} and $3.5168 \times 10^{-4} \text{ m}^2$ for the outlet area of PM2.5 (and PM1.0) impactor cups. Outlet velocity of 0.1 m/s and 0.24 m/s were obtained for PM10 and PM2.5 (and PM1.0), respectively.

2D incompressible Navier-Stokes equations were applied to validate the air flow inside the PM cup. The computation domain inside the particle size classifier of PM10, PM2.5, and PM1.0 impactors are shown in Figure 3.19 (a), (b), and (c), respectively. Air flow in three Faraday cages were validated at inside, Faraday cup's surface, and outlet. Figure 3.20 shows computational domain of three Faraday cage. The velocity of all air inside can be calculated from $v = Q / A$. For 5 L/min flow rate and all of three cages have $2.062 \times 10^{-5} \text{ m}^2$ in the outlet, which led to 4.041 m/s in air velocity.

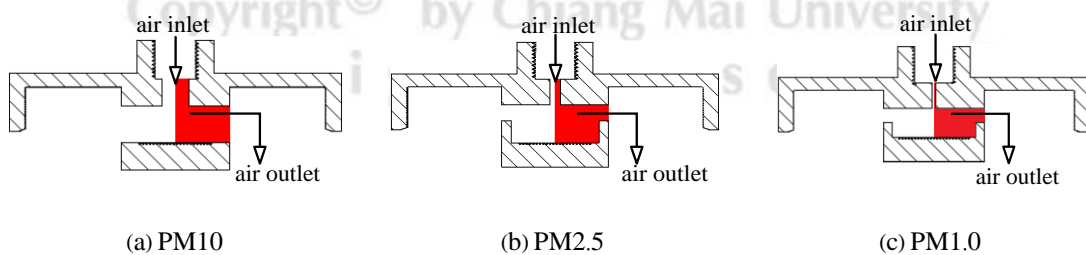


Figure 3.19 Computational domain of the inertial impactor.

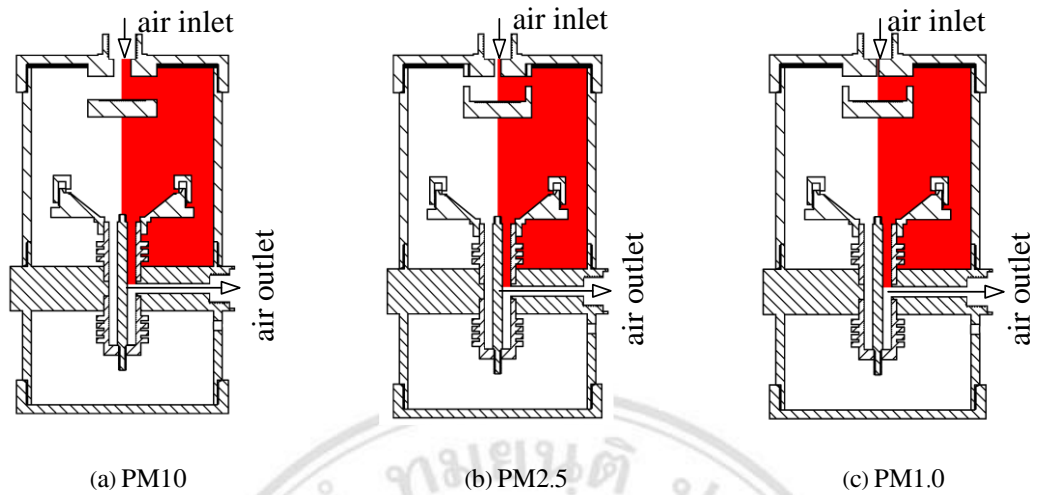


Figure 3.20 Computational domain of the Faraday cage and electrometer.

2) **Governing Equation for the Particle Trajectories.** Electric current and electrostatic field from Eqs. (2.90) to (2.94) Khan and Richardson equation from Eqs. (2.95) to (2.97) were applied to validate the particle trajectories inside the cup.

3) **Computational Domain and Boundary Condition.** Flow field in PM10, PM2.5, and PM1.0 of Faraday cages were validated by 2D incompressible Navier-Stokes equations as shown in Eqs. (2.86) to (2.89). Boundary conditions of PM10, PM2.5, and PM1.0 impactors and Faraday cages are shown in Figures 3.21 and 3.22 (a) to (c), respectively. In addition, particle trajectories inside the Faraday cage were validated by Khan-Richardson and electrostatic model equation from Eqs. (2.90) to (2.97).

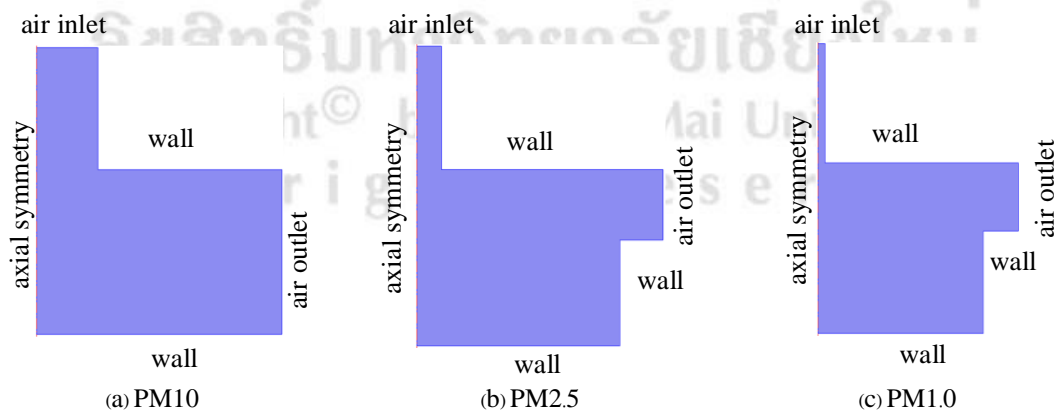


Figure 3.21 Boundary conditions of the inertial impactor.

3.5 Electrometer Circuit

3.5.1 Requirements

Faraday cage has a function to protect the electrical interference signal to the Faraday cups. It was used to install the electrometer circuit. The circuit should be near a Faraday cup. Because the particle charge has ultra-low signal about 10 fA levels, so, the electrometer must have very high amplification gain and ultra-low input bias. In addition, it should be stable, long lifetime, and affordable.

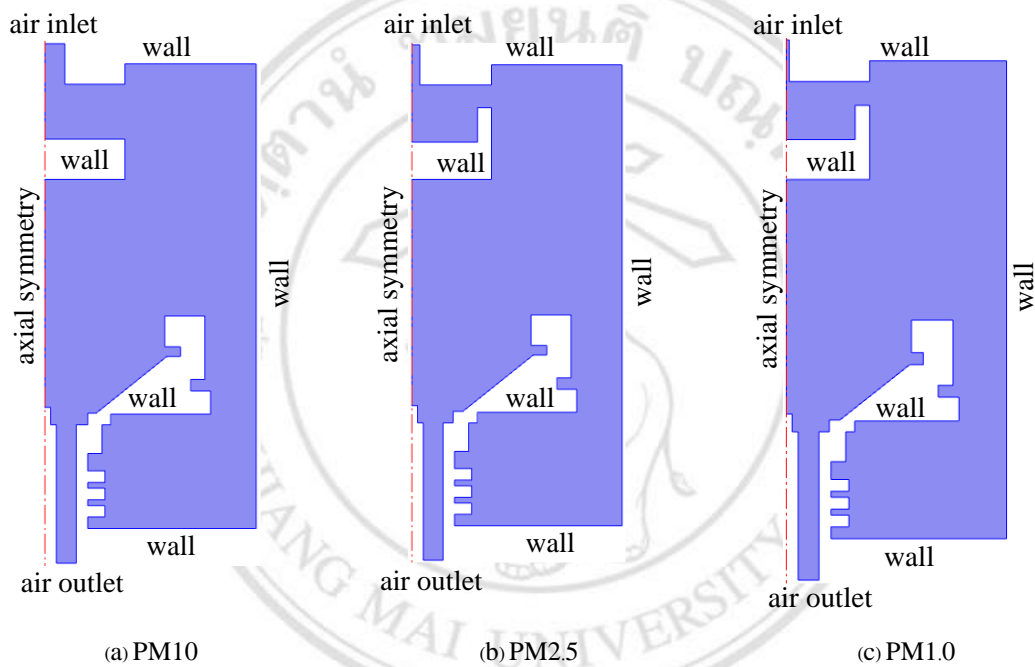


Figure 3.22 Boundary conditions of the Faraday cage.

3.5.2 Design Description

CMOS Op Amp LMC6032 was used. There were two operation amplifiers inside and an ultra-low input bias current about 40 fA. Circuit of an electrometer is shown in Figure 3.23. It was a general inverting operational amplifier circuit. The output voltage can be calculated from Eqs. (2.58) which needs to use a high resistance for feedback resistor (R_f). Diode D1N4007 was used for protecting reverse polarity of power supply and has IC7805 and IC7905 for regulating an electrical voltage. The 10 Ω resistors, 10 μ F of electrolyte capacitors and 1 μ F of polyester capacitors were used for regulating stable voltage at ± 5 VDC for pin 4 and 8 of LMC6032, respectively. The LMC6032 can be used with electric power between 5 to 15 VDC but avoid excess voltage over 16 VDC

from negative to positive which in this circuit used 10 VDC. To avoid resistance on PCB sheet, LMC 6032 and resistor were floated on air. Furthermore, the circuit was wrapped with brass, which is a Faraday cage, as shown in Figure 3.24.

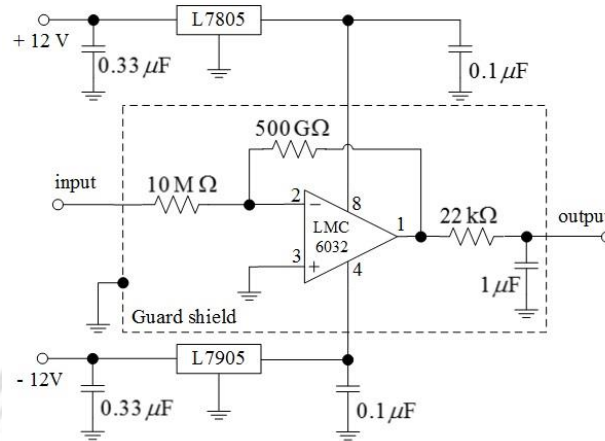


Figure 3.23 Amplifier circuit for ultra-low input signal.



Figure 3.24 Feature of the particle detector for PM10, PM2.5, and PM1.0.

3.5.3 Analytical Models

The output voltage of a basic inverting circuit was calculated from Eqs. (2.58). It had 10 mV output from 20 fA input current. In addition, RC low pass filter was applied for cutting high frequency and protecting from ripple signal. Cutoff frequency from Eqs. (3.19) can be calculated 7.23 Hz and 22 ms in time constant which was less than 1s from requirement, where R is 22 kΩ in resistance and C is 1 μF in capacitance.

$$\text{Cut off frequency} = \frac{1}{2\pi RC} \quad (3.19)$$

3.5.4 Numerical Models

The electrometer circuit as shown in Figure 3.25 was validated by Orcad PSpice software version 9.2 (student version). This software was developed by Cadence Design System, Inc., which has a high performance for validating characteristic of voltage, current, and power in the electric circuit.

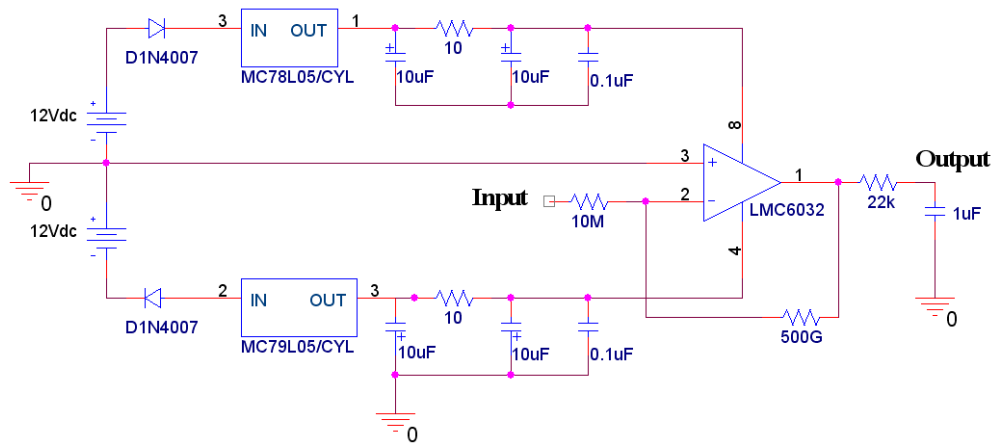


Figure 3.25 Simulation circuit of the electrometer.

3.6 Flow System

3.6.1 Requirements. Air flow is an important variable for measuring system in this thesis. The measurement result should be accurate if the air flow system is stable and accurate. It needs for stability when operated the measuring system in a long time. In addition, it can be adjustable and display the air flow rate. Particle flow in each of the channels was set at 5 L/min, so, the flow controller need to install near the impactor or the Faraday cage for a highly accurate flow rate.

3.6.2 Design Description. Main air flow had 15 L/min at the sampling head, the diffusion dryer, and the particle charger. Then the air flow was separated in three ways at 5 L/min flow rate and pass to the particle size classification in the Faraday cage. The air outlet from three Faraday cages were confluent before passing to the vacuum pump. The flow meter and controller must be installed between the Faraday cage and confluent point for protecting pressure drop and vacuum in the measuring system. Popular air flow monitor and controller are Rotameter, as shown in Figure 3.26 from Dwyer Company. It had a needle valve for adjusting air flow rate and $\pm 2\%$ full scale accuracy.



Figure 3.26 Flow meter and control.

Vacuum pump in this thesis used was diaphragm GAST model 22D1180 series (DC motor), as shown in Figure 3.27. It had 25 PSI maximum pressure, 3,200 rpm and 1.3 CFM or about 36.81 L/min flow rate (no load) at 6.2 A and 12 V of input current and voltage, respectively. Vacuum pump was connected after the Rotameter and installed on the rubble for decreasing vibration inside the measuring unit.



Figure 3.27 Feature of DC vacuum pump.

3.7 Electrical Power System

3.7.1 Requirements. The particle charger, electrometer circuit, the data acquisition, and vacuum pump require electric power for operation. The demand and levels of electric power in each device are different, but all devices must use the electric power at 12 V, same voltage levels in a battery. The battery is a good high stable electric power supply, but this measuring system designed to use a 220 VAC system and use battery for emergency case. The battery was charged an electric by the battery charger circuit and cut circuit when power full. The particle charger need to use a direct current high voltage about 3 kV and 300 V for generating and trap an ion, respectively, which the high voltage

module can control output voltage from the input voltage. The electrometer circuit needed to use a high stable of the power supply at 5 VDC on positive/ground/negative type. The data acquisition need a low voltage about 12 VDC. The vacuum pump need to use a 12 VDC low voltage, but high current about 5A. In addition, the electrical system needs to have the battery charging circuit

3.7.2 Design Description. The DC switching power supply 15 V 20A as shown in Figure 3.28 was used with the battery charging circuit as shown in Figure 3.29 for charged a battery. The particle charging device use the Spellman high voltage power supply as shown in Figure 3.30 model MM10P1.5/12 and model MM0.5P1.5/12 generated 3.0 kV and 300V in voltage for generated and trap ion, respectively. Spellman power supply can control output voltage by input voltage, which this thesis uses LM317T circuit for varying voltage input between 1.5 to 12 VDC. In addition, ICL7660SCPA and LM7805/7905 were used for generating ± 5 VDC for the electrometer circuit. The circuits of LM317T, CLM7660, LM7805 and LM7905 were shown in Figure 3.31.



Figure 3.28 DC switching power supply 220VAC 50Hz/15VDC 20A.

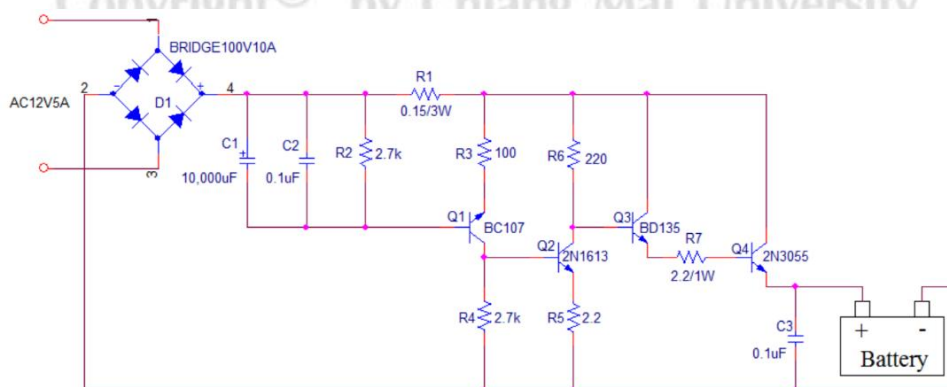


Figure 3.29 Battery charging circuit.



(a) 10kV maximum output (b) 500 V maximum output

Figure 3.30 Spellman high voltage power supply.

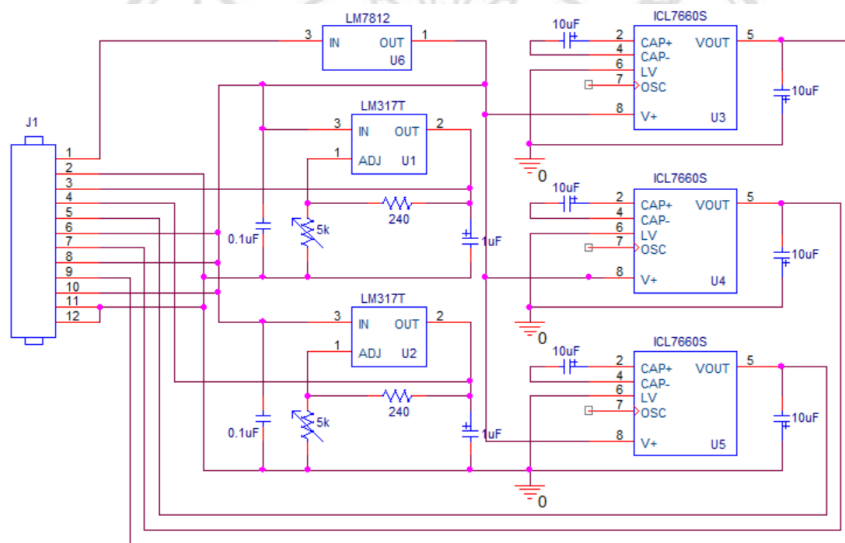


Figure 3.31 Power supply circuit for Spellman and electrometer circuit.

3.4 Data Acquisition and Processing System

3.8.1 Requirements. Electrometer circuit has an analog signal voltage between 0 to 5 VDC, so, the data acquisition required the analog to digital converter (ADC) for sending analog signal to the computer. Electrometer in this thesis had an input voltage resolution about 5 mV or 10 fA. The ADC resolution can be calculated from Eqs. (2.59). Voltage input was 5V and required 5 μ V for resolution, then the ADC required more than 12 bits and needs to have 30 to 100 ms sampling rate. Processing system was used for receiving data from the data acquisition unit. It must be able to record data, processing data and display to graph fast. In addition, it must be small, robust, low price, but high performance.

3.8.2 Design Description. This thesis used the ADAM-4017 data acquisition modules (Figure 3.32) and the UCON-485 to USB converter (Figure 3.33) for converting analog to digital data and 485 to USB port, respectively. ADAM-4017 had 8 channel inputs 16 bit data, uses 12 VDC power supply and had digital signal in RS-485 protocol output. UCON-485 can convert digital signal in RS-485 to USB port protocol. Both devices were able to work well together and can operate in a long time. The personal computer was used for processing data system. Operating software was Labview that can record measuring data and display data to graph simultaneously. Sampling data can be set from 0.1 s with 10 μ v resolution. Personal computer in this work was an ASUS eee model (Figure 3.34) which had Intel Atom and 1 GB RAM specification. Operating software in Figure 3.35 was developed from Labview. The dialog box shows the location for saving a data file in CSV format. The software will recheck last row in the data file and write date/time and measuring data from USB port at the new row continuously. The gap between the data are separated by commas and new row for new measuring data. Sampling time can be set in the software panel from 0.1 s upwards. Data file in CSV format can be open with Microsoft Excel which can separate data by a comma symbol.



Figure 3.32 ADAM-4017 data acquisition modules.



Figure 3.33 UCON-485 to USB converter.

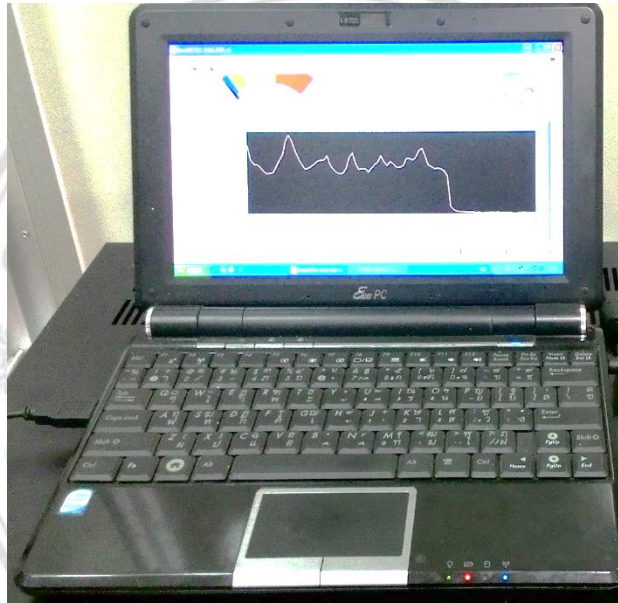


Figure 3.34 Personal computer for record PM measuring data.

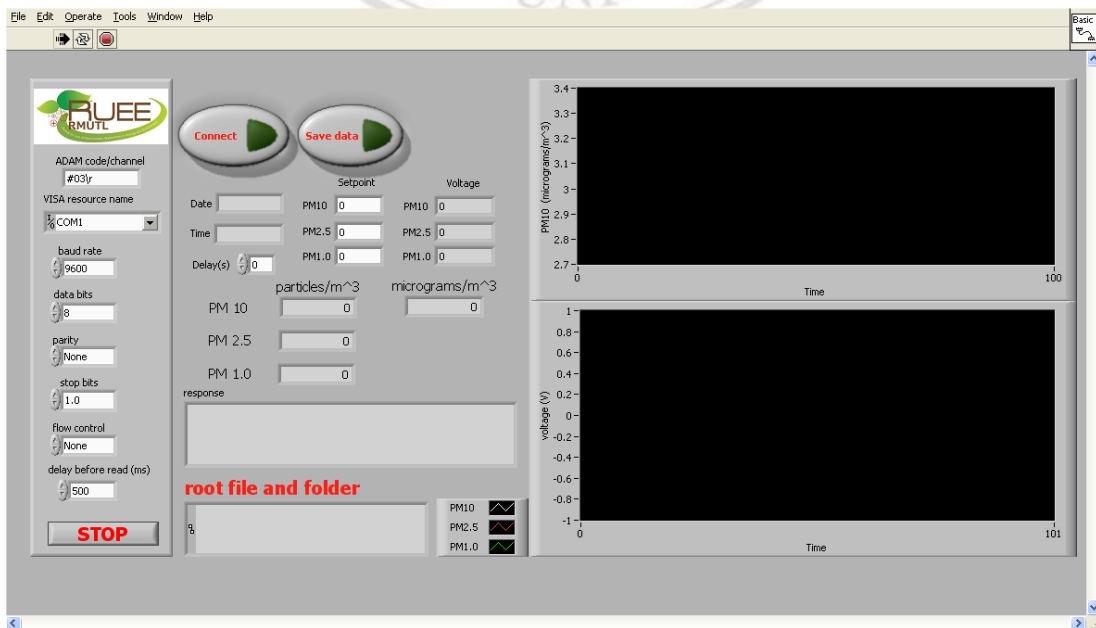


Figure 3.35 Operating software for record PM measuring data.